Nanoscale

Accepted Manuscript

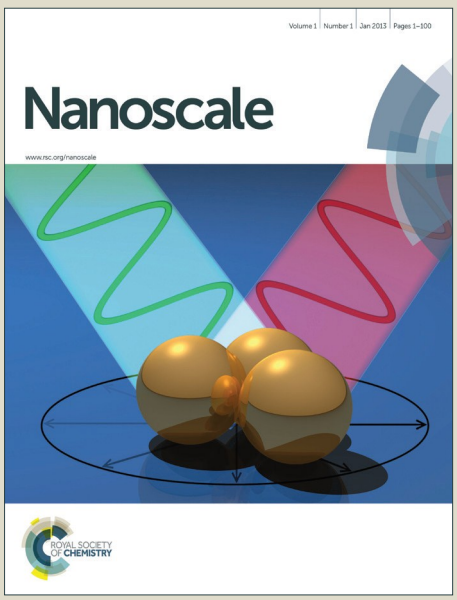

ROYAL SOCIETY OF CHEMISTRY

www.rsc.org/nanoscale

Journal Name

RSCPublishing

ARTICLE

A facile method to fabricate functionally integrated devices for oil/water separation

Cite this: DOI: 10.1039/xoxxoooooox

Qi An*,[a] Yihe Zhang*,[a] Kaikai Lv, [a] Xinglong Luan,[a] Qian Zhang[a] and Feng Shi*[b]

Received ooth January 2012,
Accepted ooth January 2012

DOI: 10.1039/xoxxoooooox

www.rsc.org/

In this paper, we present a facile method for the fabrication of a functionally integrated device, which has the multi-functions of the oil-containment boom, oil-sorption material, and water/oil-separating film, through a single immersion step in an ethanol solution of stearic acid. During the simple immersion process, the two dominant factors of superhydrophobicity, surface roughness and low-surface-energy coatings, could be accomplished simultaneously. The as-prepared functionally integrated device with superhydrophobicity/superoleophilicity displayed a lower density than that of water, such that it could float on water and act as an oil-containment boom; an efficient oil-absorbing property, which was attributed to the capillary effect caused by micrometer-sized pore structures and could be used as oil-sorption materials; a high oil/water separating efficiency which was suitable for water/oil-separating film. In this way, the functions of oil collection, absorption, and water/oil separation are integrated into one single device, and these functions could work independently, reducing the cost in terms of energy consumption and being versatile for a wide range of occasions.

Introduction

Superhydrophobic surfaces, which originated from the self-cleaning property of lotus leaves found by Barthlott and Neinhuis in 1997[1], have been a significant research topic in the fields of nanoscience and nano-sized coating materials since Jiang et al. established the concept to biomimic naturally created surfaces with specific wettability.[2-3] Inspired by the functions of natural creatures, research on superhydrophobic materials concerns practical applications of extreme surface-wetting properties for both fundamental research and industrial use, such as oil/water separation,[4-8] self-cleaning coatings,[9-11] drag reduction,[12] anti-reflection,[13] and so on. Among the various proposed applications, oil/water separation through superhydrophobic materials is highly pursued, owing to its advantages of being facile, low cost, and environmentally benign.[14-16] Until now, there has been three strategies for using superhydrophobic or underwater-superoleophobic materials for oil/water separation. The first strategy is to use superhydrophobic/superoleophilic surfaces by introducing superhydrophobicity into materials such as metal meshes, porous polymer membranes, carbon nanotube network films, and polymer–nanoparticle composites.[17-19] The second strategy is to use underwater-superoleophobic surfaces for the treatment of an oil/water mixture in the presence of a large quantity of water.[20-21] Following this principle, Jiang et al. developed a series of underwater-superoleophobic surfaces using a hydrophilic hydrogel coating,[22] a plasma-treated polydimethylsiloxane surface,[23] and a nanowire-haired copper mesh.[24] The third solution is to adjust the surface wettability between superhydrophobic and superhydrophilic in order to separate the oil and water, respectively, with the same type of membrane.[24,25] In this situation, Jiang's group reported a temperature-responsive wettability change through block copolymer coatings containing poly(N-isopropylacrylamide)[26,27] and photo-induced water/oil separation with ZnO arrays.[24,28] Similarly, Huck et al. used different pH-responsive polymer brushes in an attempt to separate oil/water mixtures.[29] Considering the fact that these smart surfaces with extreme surface wettability could only collect water or oil separately in an ex situ manner, we realized in situ continuous separation of water/oil/water ternary mixtures responding to pH stimulus, thus contributing to an increased separation efficiency.[15] However, the present work on oil/water separation mainly focuses on the single function of water/oil separation and uses the as-prepared films as separating membranes, which lose a few nano-effects of the superhydrophobic coatings. Therefore, the challenge of improving superhydrophobic coatings from the limitation of a single function to integrated multi-functions related with oil cleaning still remains.

To promote the water/oil separation application of superhydrophobic coatings from membranes with a single function to multi-functional devices, we previously proposed a strategy for the fabrication of a device that combined the multi-functions of the oil-containment boom, oil-sorption material, and water/oil-separating film;[30-31] the device could operate independently in a continuous way and the water/oil separation efficiency was as high as 98%. The fabrication of such devices involves two steps for the construction of superhydrophobic surfaces. The first step is electroless metal (gold or silver) deposition in order to obtain hierarchical rough structures; the subsequent step involves the introduction of low-surface-energy thiol species onto the rough surface. The preparation process was relatively complex and expensive, because of the step-by-

step procedures and the consumption of noble metals. To further promote the industrialization and commercialization of such functionally integrated devices, a facile and versatile fabrication method is still lacking. Therefore, in this paper, we present the fabrication of a functionally integrated device, using a facile solution-immersion process with a copper-foam substrate. The device was composed of folded copper foam, and was immersed in an ethanol solution of stearic acid for surface modification. In one single immersion step, the two dominant factors for superhydrophobicity, that is, surface roughness and low-surface-energy coatings, could be accomplished, which dramatically simplified the fabrication procedure. The as-prepared functionally integrated device with superhydrophobicity displayed a low density, such that it could float on water and act as an oil-containment boom, an efficient oil-absorbing property attributed to the capillary effect caused by micrometer-sized pore structures, and a high oil/water separating efficiency above 80%. In this way, the functions of oil collection, absorption, and water/oil separation are integrated into one single device, and these functions could work independently, reducing the cost in terms of energy consumption and being versatile for a wide range of occasions.

Experimental

Materials and instruments

Toluene, stearic acid, n-hexane, silicone oil, and Solvent Blue 78 (Sinopharm Chemical Reagent Beijing Co., Ltd., Beijing, China) were used as received. Petroleum was obtained from the Shengli Oilfield. Copper foam (Anping Xinlong Wire Mesh Manufacture Co., Ltd., China) was cleaned by alternate ultrasonication in ethanol and deionized water three times and then dried in an oven.

Scanning electron microscopy (SEM) measurements were carried out on an EVO MA25 instrument at 20.0 kV. Photographic images were taken with a Nikon camera (D5000). The contact angle was characterized using an OCA20 instrument (DataPhysics Instruments Gmbh, Filderstadt, Germany).

Fabrication of the functionally integrated device.

The device was first folded into a topless box with the intended dimensions using tweezers. Then, the topless box was immersed into a solution of 0.2 M stearic acid in ethanol for 48 h, followed by through washing with ethanol and drying in a nitrogen stream.

Separating toluene and other oils from water.

In order to distinguish toluene from water, we dyed the toluene a blue color with a solvent dye called Solvent Blue 78. The labeled toluene (50 mL) and 150 mL of water were placed in a beaker, thus forming an oil and water mixture. After the as-prepared device was put on the surface of the solution, dyed toluene rapidly infiltrated the device. We then collected the toluene in the box with a dropper and measured its volume. Other oils (n-hexane, silicone oil, and petroleum) were collected from the water surface and measured similarly.

Results and discussion

The functionally integrated device based on copper foam was folded into a cubic box (without a top) to a dimension of 2.5 × 2.5 × 1.5 cm^3. The one-step process used to obtain superhydrophobicity was realized by immersing the copper-foam cube into an ethanol solution of stearic acid (0.2 M) for 48 h at room temperature and ambient pressure, followed by sufficient washing with ethanol and drying. In order to check whether the immersion process provided enough surface roughness, we characterized the surface morphology of the copper foam before and after immersion with scanning electron microscopy (SEM). Before the immersion step, the copper-foam substrate possessed ample microscopic pores with diameters of several hundred micrometers, with some of them even approaching 1 mm, as shown in Figure 1a. The inter-pore area was the copper skeleton with a diameter of around 500 μm. The copper skeleton appeared to have a smooth surface morphology, as displayed in the enlarged SEM images in Figure 1b,c. After immersion in the ethanol solution of stearic acid, although the porous features of the copper foam changed slightly (Figure 1d), the originally smooth area of the copper skeleton gradually developed a roughness with nanoscopic dimensions over the period of 48 h (Figure S1). Nanoscopic bumps, ridges, and valleys formed on the surface of the copper skeleton, with occasional nanoscopic flowers, as shown in Figure 1e,f. The reason for the formation of the nanoscopic features on the copper skeleton was speculated to be the catalytic oxidation of copper by dissolved oxygen. Although the oxidation of copper by dissolved oxygen is usually slow, the stearic acid in the solution provided an acidic environment, which significantly accelerated the process. Thus, the nanoscopic features that formed as a result of the oxidation were readily observable within 2 days.[32] This nanoscopic roughness, in combination with the microscopic roughness provided by the copper foam, enabled the skeleton of the box to meet the geometric requirements of a superhydrophobic surface, with simultaneous microscopic and nanoscopic features.

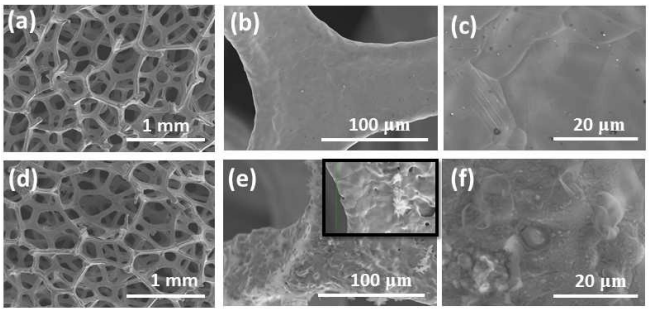

Figure 1. SEM images of (a-c) untreated copper foam and (d-f) copper foam after immersion in the solution of stearic acid for 48 h.

In addition to a rough structure, the other key factor for superhydrophobicity is the low-surface-energy coating, which was expected to be formed by a chelating effect between stearic acid and the copper surface.[32] The presence of stearic acid on the copper surface was verified by Energy Dispersive Spectrometer (EDS) characterization. As shown in Figure 2a, before the immersion step, copper was the dominant element on the surface and there were no signals detected from carbon or oxygen atoms. As metallic copper has a high surface energy, the surface wetting property of the untreated copper foam should be hydrophilic. After the immersion step, the signal of carbon and oxygen atoms, which were contained in stearic acid, appeared clearly in the EDS spectra, as shown in Figure 2b. The detailed EDS element-distribution pattern showed that the C and O atoms were distributed homogeneously on the surface

of the copper skeleton (Figure 2c–e), indicating complete coverage of the copper surface with stearic acid and the introduction of low-surface-energy coatings on the previously formed rough surface of the copper foam. Thus, the low-surface-energy coatings on the copper foam together with its hierarchical rough surface, microscale skeleton, and nanoscale structures endowed the substrate with superhydrophobic properties. After we had confirmed the rough structure and low-surface-energy coating, which were essential for superhydrophobicity, we wondered whether the substrate exhibited both superhydrophobicity and superoleophilicity, which was confirmed by contact angle (CA) measurements. The CA of the substrate for water increased gradually over the period of 48 h (Figure S2), leading to a final CA of 153.1° with a water droplet of 4 μL after immersion for 48 h. During the CA measurement with an oil droplet, the cyclohexane or toluene drop diffused into the porous walls of the substrate immediately after it made contact with the surface (Figure S3). The above CA measurements demonstrated that the device made of copper foam in stearic acid was simultaneously superhydrophobic and superoleophilic.

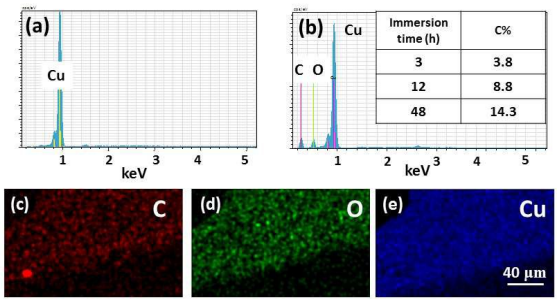

Figure 2. EDS results of (a) untreated copper foam and (b) copper foam after immersion. Element scan of (c) C, (d) O, and (e) Cu of the copper form after the solution-immersion treatment.

Although we have obtained a device with superhydrophobic and superoleophilic surfaces, whether or not the device integrated the multi-functions necessary for oil cleaning needed to be checked further. Therefore, we placed a water droplet onto the outer surface using a plastic dropper, which presented a spherical shape (Figure 3a) and rolled off rapidly (Figure 3b). This observable phenomenon matched the superhydrophobic property of the as-prepared surfaces. Owing to its superhydrophobicity, the copper-foam device could float on the water surface, which could be used as an oil-containment boom because it exhibited a lower density (0.34 g/cm^3) than water and should be suitable for usage as a floating barrier on a water surface. In addition, a drop of water placed inside the box was not able to filter through the wall of the box, but was contained inside and displayed the shape of a twisted sphere, owing to the effect of gravity and the constraint of the superhydrophobic walls of the device (Figure 3c). The reason that the device could float on water was that its superhydrophobic walls trapped ample air bubbles (defined as plastron effect[33]) and served as an air cushion, which provided extra buoyancy for the device to float on the water's surface; meanwhile, it prevented the water droplet inside the box from merging with the water outside of the device. In a clear comparison with the device that displayed superhydrophobic properties, the untreated device was hydrophilic, owing to the hydrophilic nature of the copper surface. A drop of water on the untreated substrate quickly spread and diffused into the porous walls (Figure 3d). These results demonstrated that the superhydrophobic device could provide the function of oil-containment boom, which was normally used for the quick response, collection, and recovery of offshore oil spills. For this purpose, the superhydrophobic surface with a plastron effect resulted from the bubble layer between the solid and liquid, which provided a drag-reducing effect in order to lower the fluidic friction, thus contributing to the improved movement velocity and the reduced energy consumption. This feature should be favorable for accelerating oil collection with the as-prepared device acting as an oil fence.

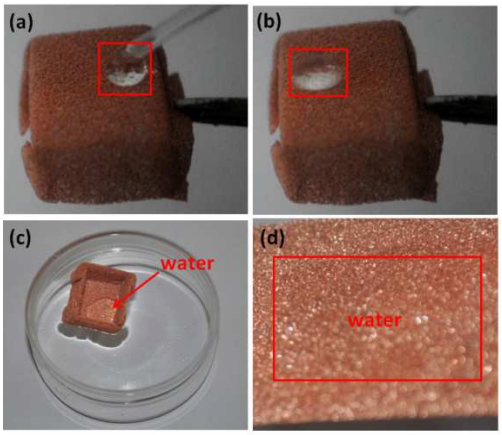

Figure 3. (a) A drop of water placed on the outer surface of the device. (b) Upon tilting the device, the drop of water slid off quickly. (c) A drop of water places inside the device. (d) A drop of water place on the surface of the untreated copper foam.

The second function anticipated from the as-prepared superhydrophobic device was a superior oil-absorption capacity, which was evaluated with a model oil droplet of toluene labelled with Solvent Blue 78 dye. From the snapshots in Figure 4a,b, we could observe that a blue oil droplet was placed on the water surface and that the device was approaching the droplet. Upon contact (Figure 4c), the oil droplet was immediately absorbed into the porous walls of the device (within seconds), without leaving any residual dyed toluene on the water surface, as displayed in Figure 4d. The efficient and selective absorption of toluene was attributed to the surface energy match between toluene and the superhydrophobic surface; meanwhile, water was rejected out of the device. In this way, the as-prepared device functioned as an oil-sorption material, which had advantages over other conventional oil-absorbing materials such as sponges, porous films, and so forth. The reason was interpreted as: 1) the highly porous structure with staggered pores at an average feature diameter of around 500 μm favored the capillary effect for absorbing liquids that could wet the surface; 2) the superoleophilic surfaces of the rough pore structures presented perfect wetting properties for oil and, thus, promoted the capillary effect for absorbing oil; and 3) the open device provided extra absorption capacity for the collected oil in addition to the loading capacity within the porous walls; moreover, by pumping away the oil in the device, the device could work in a continuous oil-absorbing way without any ex situ treatment.

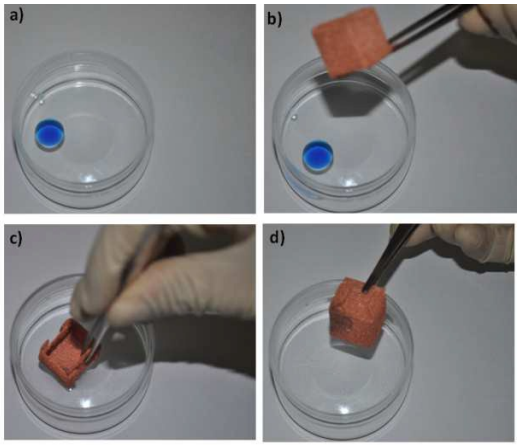

Figure 4. (a) A drop of toluene floating on a water surface. (b) The device was used to absorb the toluene droplet and, (c) upon contact, (d) the toluene droplet was absorbed into the porous walls of the device, leaving a clean water surface.

Apart from its application as an oil-absorbing material, the third function of this device is oil/water separation for the efficient removal of spilt oil from the water's surface. Taking the toluene–water system as an example, the ability of the device to continuously collect oil on a water surface was investigated, as shown in Figure 5. In this experiment, 40 mL of toluene (dyed blue) was poured onto 200 mL of water contained in a beaker; the toluene floated on top of the aqueous phase, owing to its lower density. Once the device was put into the beaker, the toluene was quickly absorbed by the device at a rate of 473 $L/(h \cdot m^2)$ and infiltrated through its walls, gathering inside the device because of the gravitational effect. The toluene that collected in the device was then transferred into the original measuring cylinder using a dropper, and the total amount collected was found to be around 38 mL. The 2 mL deficit in the collected toluene compared with the original amount was speculated to be trapped within the porous walls of the device, as evidenced by the residual blue color of the device after oil collection. Thus, the collection effect of the device was calculated to be 95%. As the amount absorbed by the device itself should be constant (the material absorb toluene to the amount of 3.5 times its own weight), the collection effect should be even greater if a larger amount of the oil phase is used in the experiment. The density of the copper foam after oil sorption was about 1.18 g/cm^3. Although the piece of copper foam after saturated oil sorption had a larger density than that of water, the device possessed extra interior volume, which contributed to overall lowered total density of the device. In this way, the device could float on the water surface when working in a continuous way to remove oil. We further tested the reusability of the device. After collecting the toluene, we washed the device with ethanol and dried with a nitrogen flow. Then, the device was reused to collect toluene once again. The process was repeated five times, and the collection efficiency was above 90% each time. The average collection efficiency over the five repeated experiments was calculated to be 92%. The average water content of the collected toluene was 0.090 w.t.%. In addition, in order to examine the durability of the device in a corrosive environment, we submerged the device into acidic water (pH 3, adjusted using HCl), basic water (pH 12, adjusted using NaOH), and salt water (0.1M NaCl solution), and measured the CAs of the substrates. The CAs remained above 140° for up to 2 days, demonstrating satisfactory stability in such corrosive environments. The pressure the device can hold was then evaluated. When the water pressure increased to 40 kPa (about 4-m depth), the superhydrophobicity was still maintained; besides, the water/oil separating property was not affected. This result meant when putting into practical use on ocean surface, the as-prepared device could resist pressure from sea wave to ensure its use.

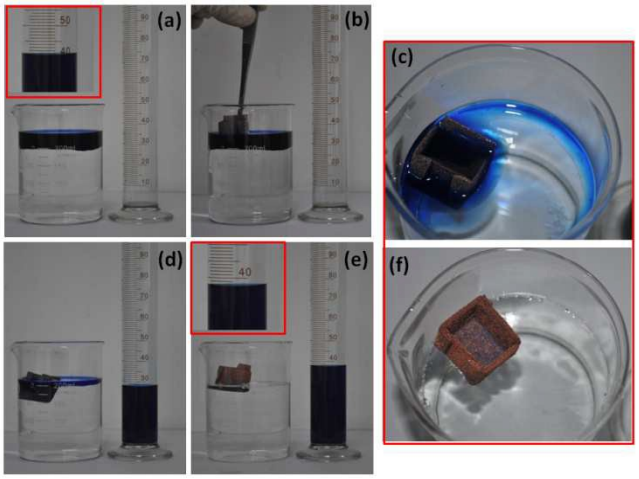

Figure 5. (a) 40 mL of toluene (dyed blue) were added to the aqueous phase and (b) the device was used to collect the toluene. A dropper was used to remove the toluene and put it back into the original measuring cylinder. (c) Toluene on the water surface continuously flowed into the device due to the gravitational effect and (d) with the removal of the collected toluene with a dropper, more toluene was collected. (e) Eventually, all the toluene was removed from the water surface, and 38 mL of toluene was collected in the original cylinder. (f) After collecting the toluene, the device floated on water surface and the porous walls of the device were dyed blue by residual toluene.

Considering the growing number of oil-spill accidents and the variable composition of oils, the collection device should be able to collect multiple types of oil from the surface of water. Therefore, we extended the collection experiment to several other organic solvents, including n-hexane, silicone oil, and petroleum. The experiments were conducted in the continuous absorption-and-pumping manner described above. For each type of organic solvent, the collection efficiency was over 80%, and even over 90% for some of them, as shown in Figure 6. The collection efficiencies were determined by averaging three parallel experiments. The deficit in the collected amount of oil compared with the original amount was mostly absorbed by the device itself, and a small amount was left inside the dropper. No evidence indicated that there was oil residue on the water surface after collection. The residual oil that was absorbed into the porous walls of the device could be washed away by ethanol and the device could be reused. The collection efficiency of the device was very high and could be enhanced further if a larger amount of oil was to be collected. The above results, in combination with the fact that the device was fabricated in both a facile and continuous absorption-and-pumping manner is applicable at larger operational scales, suggest the possibility that this device could be used in industrial applications.

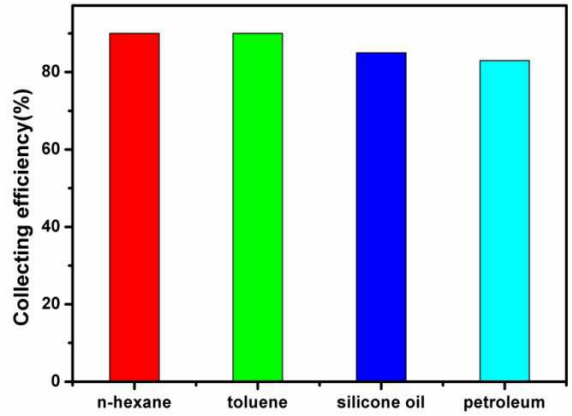

Figure 6. Collection efficiencies of the device for n-hexane, toluene, silicone oil, and petroleum (all larger than 80%).

Conclusions

In conclusion, we have achieved a functionally integrated device for the collection of oil from a water surface through a one-step solution-immersion process. The solution-immersion step provided the device with micro-/nanoscopic roughness and a low-surface-energy coating, both of which are indispensable for the construction of a superhydrophobic surface. Compared with previously reported strategies, this strategy is much easier to carry out and, in the meantime, allows the collection of oil in a continuous manner. We believe that this report will bring the construction of functionally integrated oil-collection devices a step closer to industrial applications.

Acknowledgements

This work was supported by the NSFC (21303169), the Fundamental Research Funds for the Central Universities (2652013115), Beijing Nova Program (Z141103001814064), Beijing Specific Project to Foster Elitist (2013D009015000001), the Open Project of State Key Laboratory of Chemical Resource Engineering (CRE-2013-C-201), and National High Technology Research and Development Program of China (863 Program 2012AA06A109) and the special co-construction project of Beijing city education committee.

Notes and references

[a] Beijing Key Laboratory of Materials Utilization of Nonmetallic Minerals and Solid Wastes, National Laboratory of Mineral Materials, School of Materials Science and Technology, China University of Geosciences, Beijing, 100083.

[b] Beijing Engineering Research Center for the Synthesis and Applications of Waterborne Polymers, Beijing University of Chemical Technology, Beijing 100029, PR China

E-mail: (Q.A.) an@cugb.edu.cn; (Y.Z.)zyh@cugb.edu.cn; (F.S.)shi@mail.buct.edu.cn

1 W. Barthlott and C. Neinhuis, *Planta*, 1997, **202,** 1.

2 S. Wang, H. Liu, D. Liu, X. Ma, X. Fang and L. Jiang, *Angew. Chem. Int. Ed.*, 2007, **46,** 3915.

3 L. Feng, S. Li, Y. Li, H. Li, L. Zhang and J. Zhai, *Adv Mater*, 2002, **14,** 1857.

4 L. Feng, Z. Y. Zhang, Z. H. Mai, Y. M. Ma, B. Q. Liu, L. Jiang and D. B. Zhu, *Angew. Chem. Int. Ed.* 2004, **43,** 2012.

5 Z. X. Xue, S. T. Wang, L Lin, L. Chen, M. J. Liu, L. Feng and L. Jiang, *Adv. Mater.* 2011, **23,** 4270.

6 L. B. Zhang, Z. H. Zhang and P. Wang, *NPG Asia Mater.,* 2012, **4,** e8.

7 C. H. Xue, P. T. Ji, P. Zhang, Y. R. Li and S. T. Jia, *Appl. Surf. Sci.* 2013, **284,** 464.

8 Z. Niu , L. Liu , L. Zhang , and X. Chen, Small, 2014, 10, 3434.

9 Y. W. Wu, T. Hang, Z. Y. Yu, L. Xu and M. Li, *Chem. Commun.* 2014, **50,** 8405.

10 S. Nishimoto and B. Bhushan, *RSC Adv*. 2013, **3,** 671.

11 X. Deng, L. Mammen, H. J. Butt and D. Vollmer, *Science*, 2012, **335,** 67.

12 H. Y. Dong, M. J. Cheng, Y. J. Zhang, H. Wei and F. Shi, *J. Mater. Chem. A*, 2013, **1,** 5886.

13 L. B. Zhang, Y. Li, J. Q. Sun and J. C. Shen, *Langmuir* 2008, **24,** 10851.

14 W. B. Zhang, Z. Shi, F. Zhang, X. Liu, J. Jin and L. Jiang, *Adv. Mater.* 2013, **25,** 2071.

15 G. N. Ju, M. J. Cheng and F. Shi, *NPG Asia Mater.* 2014, **6,** e111.

16 M. J. Cheng, G. N. Ju, C. Jiang, Y. J. Zhang and F. Shi, *J. Mater. Chem. A*, 2013, **1,** 13411.

17 C. X. Wang; T. J. Yao; J. Wu; C. Ma; Z. X. Fan; Z. Wang; Y. R. Cheng; Q. Lin and B. Yang, *ACS Appl. Mater. Interfaces* 2009, **1**, 2613.

18 Q. M. Pan, M. Wang and H. B. Wang, *Appl. Surf. Sci.* 2008, **254,** 6002.

19 A. K. Kota, G. Kwon, W. Choi, J. M. Mabry and A. Tuteja, *Nat. Commun.* 2012, **3,** 1025.

20 M. Gui, J. Orozco, M. Garcia, W. Gao, S. Sattayasamitsathit, A. Merkoci, A. Escarpa and J. Wang, *ACS Nano* 2012, **5,** 4445.

21 K. Li, J. Ju, Z. X, Xue, J. Ma, L. Feng, S. Gao and L. Jiang *Nat. Commun.* 2013, **4,** 2276.

22 Z. Xue, S. Wang and L. Lin, *Adv. Mater.,* 2011, **23,** 4270.

23 M. Tao, L. Xue and F. Liu, *Adv. Mater.,* 2014, **26,** 2943.

24 D. Tian, Z. Guo, Y. Wang, W. Li, X. Zhang, J. Zhai and L. Jiang, *Adv. Funct. Mater.,* 2014, **24,** 536.

25 G. Ju, M. Cheng, M. Xiao, J. Xu, K. Pan, X. Wang, Y. Zhang and F. Shi, *Adv. Mater.,* 2013, **25,** 2915.

26 T. Zhao, F. Nie and L. Jiang, *J. Mater. Chem.* 2010, **20,** 2176.

27 L. Chen, M. Liu, L. Lin, T. Zhang, J. Ma, Y. Song and L. Jiang, *Soft Matter,* 2010, **6,** 2708.

28 D. Tian, X. Zhang, Y. Tian, Y. Wu, X. Wang, J. Zhai and L.Jiang, *J. Mater. Chem.* 2012, **22,** 19652.

29 K. Tan, T. Hughes, M. Nagl and W. Huck, *ACS Applied Mater. & Interfaces,* 2012, **4,** 6403.

30 M. Cheng, Y. Gao, X. Guo, Z. Shi, J. Chen and F. Shi, *Langmuir* 2011, **27,** 7371.

31 M. Cheng, G. Ju, C. Jiang, Y. Zhang and F. Shi, *J. Mater. Chem. A,* 2013, **1,** 13411.

32 S. T. Wang, L. Feng and L. Jiang, *Adv. Mater.* 2006, **18,** 767.

33 G. McHale, M. R. Flynn and M. I. Newton, *Soft Matter* 2011, **7,** 10100.